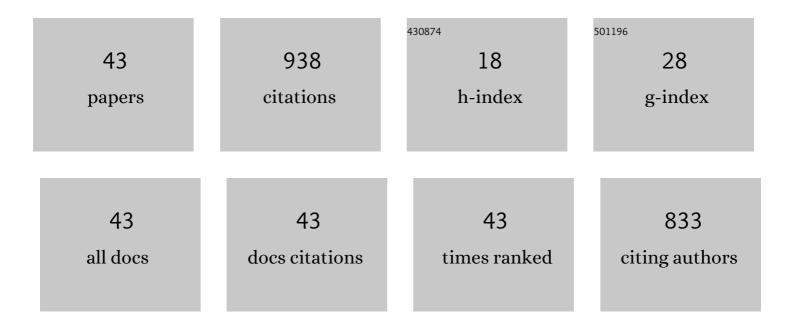
## Changxun Yu

List of Publications by Year in descending order

Source: https://exaly.com/author-pdf/2698834/publications.pdf Version: 2024-02-01



#	Article	IF	CITATIONS
1	Extensive dispersion of metals from hemiboreal acid sulfate soil into adjacent drain and wetland. Applied Geochemistry, 2022, 136, 105170.	3.0	4
2	A re-assessment of metal pollution in the Dexing mining area in Jiangxi province, China: current status, hydro-geochemical controls, and effectiveness of remediation practices. International Journal of Environmental Science and Technology, 2022, 19, 10707-10722.	3.5	6
3	High potential of stable carbon sequestration in phytoliths of China's grasslands. Global Change Biology, 2022, 28, 2736-2750.	9.5	23
4	Removal and potential recovery of dissolved metals from acid sulfate soil drainage by spent coffee-grounds and dissolved organic carbon. Environmental Advances, 2022, 8, 100193.	4.8	4
5	The response of metal mobilization and redistribution to reoxygenation in Baltic Sea anoxic sediments. Science of the Total Environment, 2022, 837, 155809.	8.0	4
6	Arsenic in the water and agricultural crop production system: Bangladesh perspectives. Environmental Science and Pollution Research, 2022, 29, 51354-51366.	5.3	16
7	Storage, patterns and influencing factors for soil organic carbon in coastal wetlands of China. Global Change Biology, 2022, 28, 6065-6085.	9.5	29
8	Distribution, sources, and decomposition of soil organic matter along a salinity gradient in estuarine wetlands characterized by C:N ratio, l´ <sup>13</sup> Câ€í <sup>15</sup> N, and lignin biomarker. Global Change Biology, 2021, 27, 417-434.	9.5	63
9	Vertical distributions of organic carbon fractions under paddy and forest soils derived from black shales: Implications for potential of long-term carbon storage. Catena, 2021, 198, 105056.	5.0	15
10	Vegetation Determines Lake Sediment Carbon Accumulation during Holocene in the Forest–Steppe Ecotone in Northern China. Forests, 2021, 12, 696.	2.1	6
11	Biogeochemical cycling of iron (hydr-)oxides and its impact on organic carbon turnover in coastal wetlands: A global synthesis and perspective. Earth-Science Reviews, 2021, 218, 103658.	9.1	47
12	Spatial distribution of plant-available silicon and its controlling factors in paddy fields of China. Geoderma, 2021, 401, 115215.	5.1	16
13	Microbe-Mediated Mn Oxidation—A Proposed Model of Mineral Formation. Minerals (Basel,) Tj ETQq1 1 0.784	314 rgBT 2.0	Overlock 10/
14	Quantification of different silicon fractions in broadleaf and conifer forests of northern China and consequent implications for biogeochemical Si cycling. Geoderma, 2020, 361, 114036.	5.1	18
15	Phytolith-rich straw application and groundwater table management over 36Âyears affect the soil-plant silicon cycle of a paddy field. Plant and Soil, 2020, 454, 343-358.	3.7	34
16	Silicon Effects on Biomass Carbon and Phytolith-Occluded Carbon in Grasslands Under High-Salinity Conditions. Frontiers in Plant Science, 2020, 11, 657.	3.6	15
17	Carbon-nitrogen isotope coupling of soil organic matter in a karst region under land use change, Southwest China. Agriculture, Ecosystems and Environment, 2020, 301, 107027.	5.3	108
18	Holocene carbon accumulation in lakes of the current east Asian monsoonal margin: Implications under a changing climate. Science of the Total Environment, 2020, 737, 139723.	8.0	7

Changxun Yu

#	Article	IF	CITATIONS
19	A review of carbon isotopes of phytoliths: implications for phytolith-occluded carbon sources. Journal of Soils and Sediments, 2020, 20, 1811-1823.	3.0	6
20	Storage of soil phytoliths and phytolith-occluded carbon along a precipitation gradient in grasslands of northern China. Geoderma, 2020, 364, 114200.	5.1	16
21	A Combined X-ray Absorption and Mössbauer Spectroscopy Study on Fe Valence and Secondary Mineralogy in Granitoid Fracture Networks: Implications for Geological Disposal of Spent Nuclear Fuels. Environmental Science & Technology, 2020, 54, 2832-2842.	10.0	10
22	Silicon accumulation controls carbon cycle in wetlands through modifying nutrients stoichiometry and lignin synthesis of Phragmites australis. Environmental and Experimental Botany, 2020, 175, 104058.	4.2	19
23	Silicon Affects Plant Stoichiometry and Accumulation of C, N, and P in Grasslands. Frontiers in Plant Science, 2020, 11, 1304.	3.6	16
24	Comparison of boreal acid sulfate soil microbial communities in oxidative and reductive environments. Research in Microbiology, 2019, 170, 288-295.	2.1	8
25	Geochemical controls on dispersion of U and Th in Quaternary deposits, stream water, and aquatic plants in an area with a granite pluton. Science of the Total Environment, 2019, 663, 16-28.	8.0	6
26	Micro-scale isotopic variability of low-temperature pyrite in fractured crystalline bedrock ― A large Fe isotope fractionation between Fe(II)aq/pyrite and absence of Fe-S isotope co-variation. Chemical Geology, 2019, 522, 192-207.	3.3	3
27	Impact of grassland degradation on the distribution and bioavailability of soil silicon: Implications for the Si cycle in grasslands. Science of the Total Environment, 2019, 657, 811-818.	8.0	29
28	A cryogenic XPS study of Ce fixation on nanosized manganite and vernadite: Interfacial reactions and effects of fulvic acid complexation. Chemical Geology, 2018, 483, 304-311.	3.3	14
29	Sources, transport and sinks of beryllium in a coastal landscape affected by acidic soils. Geochimica Et Cosmochimica Acta, 2018, 232, 288-302.	3.9	26
30	Cerium sequestration and accumulation in fractured crystalline bedrock: The role of Mn-Fe (hydr-)oxides and clay minerals. Geochimica Et Cosmochimica Acta, 2017, 199, 370-389.	3.9	43
31	Fluorine geochemistry of quaternary deposits in a nemo-boreal catchment with elevated dissolved fluoride in surface waters and groundwater. Journal of Geochemical Exploration, 2016, 170, 148-156.	3.2	10
32	Manganese accumulation and solid-phase speciation in a 3.5 m thick mud sequence from the estuary of an acidic and Mn-rich creek, northern Baltic Sea. Chemical Geology, 2016, 437, 56-66.	3.3	12
33	Distribution and speciation of metals, phosphorus, sulfate and organic material in brackish estuary water affected by acid sulfate soils. Applied Geochemistry, 2016, 66, 264-274.	3.0	31
34	Arsenic removal from contaminated brackish sea water by sorption onto Al hydroxides and Fe phases mobilized by land-use. Science of the Total Environment, 2016, 542, 923-934.	8.0	13
35	Iron behavior in a northern estuary: Large pools of non-sulfidized Fe(II) associated with organic matter. Chemical Geology, 2015, 413, 73-85.	3.3	26
36	Geochemistry of major and trace elements and Pb–Sr isotopes of a weathering profile developed on the Lower Cambrian black shales in central Hunan, China. Applied Geochemistry, 2014, 51, 191-203.	3.0	34

Changxun Yu

#	Article	IF	CITATIONS
37	Retention and transport of arsenic, uranium and nickel in a black shale setting revealed by a long-term humidity cell test and sequential chemical extractions. Chemical Geology, 2014, 363, 134-144.	3.3	35
38	Geochemistry of soils derived from black shales in the Ganziping mine area, western Hunan, China. Environmental Earth Sciences, 2013, 70, 175-190.	2.7	27
39	Effect of weathering on abundance and release of potentially toxic elements in soils developed on Lower Cambrian black shales, P. R. China. Environmental Geochemistry and Health, 2012, 34, 375-390.	3.4	48
40	Geochemistry of trace metals and Pb isotopes of sediments from the lowermost Xiangjiang River, Hunan Province (P. R. China): implications on sources of trace metals. Environmental Earth Sciences, 2011, 64, 1455-1473.	2.7	32
41	Heavy metal geochemistry of the acid mine drainage discharged from the Hejiacun uranium mine in central Hunan, China. Environmental Geology, 2009, 57, 421-434.	1.2	29
42	Mineralogical and geochemical constraints on environmental impacts from waste rock at Taojiang Mn-ore deposit, central Hunan, China. Environmental Geology, 2007, 52, 1277-1296.	1.2	23
43	Soil silicon fractions along karst hillslopes of southwestern China. Journal of Soils and Sediments, 0, , 1.	3.0	1